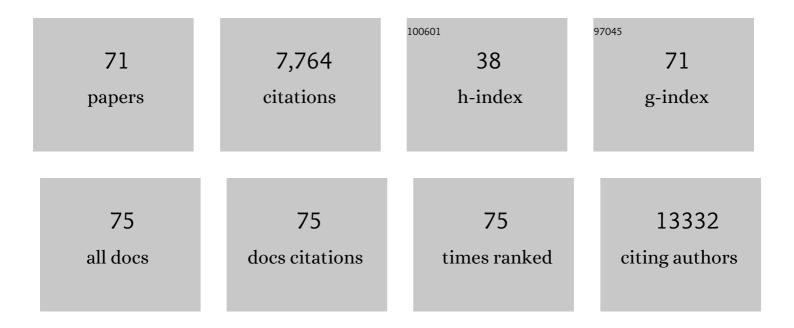
## Binghui Wu

List of Publications by Year in descending order

Source: https://exaly.com/author-pdf/9103783/publications.pdf Version: 2024-02-01



Віленці Ші

#	Article	lF	CITATIONS
1	Scalable Preparation of Highâ€Performance ZnO–SnO <sub>2</sub> Cascaded Electron Transport Layer for Efficient Perovskite Solar Modules. Solar Rrl, 2022, 6, 2100639.	3.1	13
2	Fire-resistant plant fiber sponge enabled by highly thermo-conductive hexagonal boron nitride ink. Chemical Engineering Journal, 2022, 429, 132135.	6.6	1
3	Intermediate Chemistry of Halide Perovskites: Origin, Evolution, and Application. Journal of Physical Chemistry Letters, 2022, 13, 1765-1776.	2.1	23
4	Antioxidant high-conductivity copper paste for low-cost flexible printed electronics. Npj Flexible Electronics, 2022, 6, .	5.1	21
5	Design Strategies of Hole Transport Materials by Electronic and Steric Controls for nâ€iâ€p Perovskite Solar Cells. ChemSusChem, 2022, , .	3.6	5
6	Synergistic Effect between NiO <i><sub>x</sub></i> and P3HT Enabling Efficient and Stable Hole Transport Pathways for Regular Perovskite Photovoltaics. Advanced Functional Materials, 2022, 32, .	7.8	17
7	Crown Etherâ€Assisted Growth and Scaling Up of FACsPbI <sub>3</sub> Films for Efficient and Stable Perovskite Solar Modules. Advanced Functional Materials, 2021, 31, 2008760.	7.8	50
8	Hyperstable Perovskite Solar Cells Without Ion Migration and Metal Diffusion Based on ZnS Segregated Cubic ZnTiO <sub>3</sub> Electron Transport Layers. Solar Rrl, 2021, 5, 2000654.	3.1	13
9	An Organic–Inorganic Hybrid Electrolyte as a Cathode Interlayer for Efficient Organic Solar Cells. Angewandte Chemie - International Edition, 2021, 60, 8526-8531.	7.2	54
10	An Organic–Inorganic Hybrid Electrolyte as a Cathode Interlayer for Efficient Organic Solar Cells. Angewandte Chemie, 2021, 133, 8607-8612.	1.6	16
11	Perovskite Quantum Dots as Multifunctional Interlayers in Perovskite Solar Cells with Dopant-Free Organic Hole Transporting Layers. Journal of the American Chemical Society, 2021, 143, 5855-5866.	6.6	59
12	Sulfonate-Assisted Surface Iodide Management for High-Performance Perovskite Solar Cells and Modules. Journal of the American Chemical Society, 2021, 143, 10624-10632.	6.6	101
13	Hexagonal Nickel as a Highly Durable and Active Catalyst for Hydrogen Evolution. ACS Catalysis, 2021, 11, 8798-8806.	5.5	12
14	Mo-Decorated Ni <sub>3</sub> N Nanostructures for Alkaline Polymer Electrolyte Fuel Cells. ACS Applied Nano Materials, 2021, 4, 11473-11479.	2.4	9
15	Interface Engineering of Cubic Zinc Metatitanate as an Excellent Electron Transport Material for Stable Perovskite Solar Cells. Solar Rrl, 2020, 4, 1900533.	3.1	12
16	Surface coordination layer passivates oxidation of copper. Nature, 2020, 586, 390-394.	13.7	154
17	Highly Anisotropic Corncob as an Efficient Solar Steam-Generation Device with Heat Localization and Rapid Water Transportation. ACS Applied Materials & Interfaces, 2020, 12, 50397-50405.	4.0	51
18	Sensitive piezoresistive sensors using ink-modified plant fiber sponges. Chemical Engineering Journal, 2020, 401, 126029.	6.6	22

Вілсниі Wu

#	Article	IF	CITATIONS
19	Constructing hydrophobic interfaces in aluminophosphate adhesives with reduced graphene oxide to improve the performance of wood-based boards. Composites Part B: Engineering, 2020, 198, 108168.	5.9	12
20	Methylamine-Dimer-Induced Phase Transition toward MAPbl <sub>3</sub> Films and High-Efficiency Perovskite Solar Modules. Journal of the American Chemical Society, 2020, 142, 6149-6157.	6.6	59
21	Moisture-tolerant and high-quality α-CsPbl <sub>3</sub> films for efficient and stable perovskite solar modules. Journal of Materials Chemistry A, 2020, 8, 9597-9606.	5.2	62
22	Protecting the Nanoscale Properties of Ag Nanowires with a Solution-Grown SnO <sub>2</sub> Monolayer as Corrosion Inhibitor. Journal of the American Chemical Society, 2019, 141, 13977-13986.	6.6	45
23	Ultrasensitive label-free detection of circulating tumor cells using conductivity matching of two-dimensional semiconductor with cancer cell. Biosensors and Bioelectronics, 2019, 142, 111520.	5.3	30
24	<i>N</i> -Methyl-2-pyrrolidone as an excellent coordinative additive with a wide operating range for fabricating high-quality perovskite films. Inorganic Chemistry Frontiers, 2019, 6, 2458-2463.	3.0	26
25	Existence of Ligands within Sol–Gel-Derived ZnO Films and Their Effect on Perovskite Solar Cells. ACS Applied Materials & Interfaces, 2019, 11, 43116-43121.	4.0	28
26	Intimate Interfacial Interaction between Aminoâ€Modified Ti <sub>5</sub> Clusters and BiVO <sub>4</sub> towards Efficient Photoelectrochemical Water Splitting. ChemNanoMat, 2019, 5, 1110-1114.	1.5	6
27	Br-containing alkyl ammonium salt-enabled scalable fabrication of high-quality perovskite films for efficient and stable perovskite modules. Journal of Materials Chemistry A, 2019, 7, 26849-26857.	5.2	40
28	Copper-copper iodide hybrid nanostructure as hole transport material for efficient and stable inverted perovskite solar cells. Science China Chemistry, 2019, 62, 363-369.	4.2	36
29	High-Efficiency, Hysteresis-Less, UV-Stable Perovskite Solar Cells with Cascade ZnO–ZnS Electron Transport Layer. Journal of the American Chemical Society, 2019, 141, 541-547.	6.6	189
30	Efficient, Hysteresisâ€Free, and Stable Perovskite Solar Cells with ZnO as Electronâ€Transport Layer: Effect of Surface Passivation. Advanced Materials, 2018, 30, 1705596.	11.1	363
31	Hierarchical Lamellar Aluminophosphate Materials with Porosity as Ecofriendly Inorganic Adhesive for Wood-Based Boards. ACS Sustainable Chemistry and Engineering, 2018, 6, 6273-6280.	3.2	35
32	Thiol Treatment Creates Selective Palladium Catalysts for Semihydrogenation of Internal Alkynes. CheM, 2018, 4, 1080-1091.	5.8	145
33	Electrochemical Reduction of Carbon Dioxide to Methanol on Hierarchical Pd/SnO <sub>2</sub> Nanosheets with Abundant Pd–O–Sn Interfaces. Angewandte Chemie, 2018, 130, 9619-9623.	1.6	24
34	Plant Sunscreen and Co(II)/(III) Porphyrins for UVâ€Resistant and Thermally Stable Perovskite Solar Cells: From Natural to Artificial. Advanced Materials, 2018, 30, e1800568.	11.1	114
35	Electrochemical Reduction of Carbon Dioxide to Methanol on Hierarchical Pd/SnO <sub>2</sub> Nanosheets with Abundant Pd–O–Sn Interfaces. Angewandte Chemie - International Edition, 2018, 57, 9475-9479.	7.2	218
36	Microwaveâ€Assisted Synthesis of Ultrastable Cu@TiO <sub>2</sub> Coreâ€Shell Nanowires with Tunable Diameters via a Redoxâ€Hydrolysis Synergetic Process. ChemNanoMat, 2018, 4, 914-918.	1.5	8

Вілсниї Wu

#	Article	IF	CITATIONS
37	A cake making strategy to prepare reduced graphene oxide wrapped plant fiber sponges for high-efficiency solar steam generation. Journal of Materials Chemistry A, 2018, 6, 14571-14576.	5.2	84
38	Biological responses to core–shell-structured Fe <sub>3</sub> O <sub>4</sub> @SiO <sub>2</sub> -NH <sub>2</sub> nanoparticles in rats by a nuclear magnetic resonance-based metabonomic strategy. International Journal of Nanomedicine, 2018, Volume 13, 2447-2462.	3.3	7
39	Double‣ayered Plasmonic–Magnetic Vesicles by Selfâ€Assembly of Janus Amphiphilic Gold–Iron(II,III) Oxide Nanoparticles. Angewandte Chemie - International Edition, 2017, 56, 8110-8114.	7.2	107
40	Double‣ayered Plasmonic–Magnetic Vesicles by Selfâ€Assembly of Janus Amphiphilic Gold–Iron(II,III) Oxide Nanoparticles. Angewandte Chemie, 2017, 129, 8222-8226.	1.6	25
41	Carbon nitride supported AgPd alloy nanocatalysts for dehydrogenation of formic acid under visible light. Journal of Materials Chemistry A, 2017, 5, 6382-6387.	5.2	52
42	Improving Efficiency and Stability of Perovskite Solar Cells by Modifying Mesoporous TiO <sub>2</sub> –Perovskite Interfaces with Both Aminocaproic and Caproic acids. Advanced Materials Interfaces, 2017, 4, 1700897.	1.9	41
43	Ultrastable atomic copper nanosheets for selective electrochemical reduction of carbon dioxide. Science Advances, 2017, 3, e1701069.	4.7	211
44	Air-promoted selective hydrogenation of phenol to cyclohexanone at low temperature over Pd-based nanocatalysts. Science China Chemistry, 2017, 60, 1444-1449.	4.2	11
45	Photochemical route for synthesizing atomically dispersed palladium catalysts. Science, 2016, 352, 797-800.	6.0	1,540
46	Plasmonâ€Mediated Photocatalytic Decomposition of Formic Acid on Palladium Nanostructures. Advanced Optical Materials, 2016, 4, 1041-1046.	3.6	32
47	Anisotropic Growth of TiO <sub>2</sub> onto Gold Nanorods for Plasmon-Enhanced Hydrogen Production from Water Reduction. Journal of the American Chemical Society, 2016, 138, 1114-1117.	6.6	422
48	Interfacial electronic effects control the reaction selectivity of platinum catalysts. Nature Materials, 2016, 15, 564-569.	13.3	548
49	Uniform Concave Polystyrene-Carbon Core–Shell Nanospheres by a Swelling Induced Buckling Process. Journal of the American Chemical Society, 2015, 137, 9772-9775.	6.6	53
50	A nanoparticulate polyacetylene-supported Pd(II) catalyst combining the advantages of homogeneous and heterogeneous catalysts. Chinese Journal of Catalysis, 2015, 36, 1560-1572.	6.9	8
51	Facile synthesis of size-tunable ZIF-8 nanocrystals using reverse micelles as nanoreactors. Science China Chemistry, 2014, 57, 141-146.	4.2	39
52	Amphiphilic modification and asymmetric silica encapsulation of hydrophobic Au–Fe <sub>3</sub> O <sub>4</sub> dumbbell nanoparticles. Chemical Communications, 2014, 50, 174-176.	2.2	35
53	A hydride-induced-reduction strategy for fabricating palladium-based core–shell bimetallic nanocrystals. Nanoscale, 2014, 6, 6798.	2.8	22
54	Electrostatic Self-Assembling Formation of Pd Superlattice Nanowires from Surfactant-Free Ultrathin Pd Nanosheets. Journal of the American Chemical Society, 2014, 136, 12856-12859.	6.6	66

Вілсниі Wu

#	Article	IF	CITATIONS
55	Integrated approach to evaluating the toxicity of novel cysteine-capped silver nanoparticles to Escherichia coli and Pseudomonas aeruginosa. Analyst, The, 2014, 139, 954-963.	1.7	40
56	Solvent effect on the synthesis of monodisperse amine-capped Au nanoparticles. Chinese Chemical Letters, 2013, 24, 457-462.	4.8	55
57	Supported monodisperse Pt nanoparticles from [Pt3(CO)3(μ2-CO)3]52â^ clusters for investigating support–Pt interface effect in catalysis. Dalton Transactions, 2013, 42, 12699.	1.6	27
58	Crystal structure of a luminescent thiolated Ag nanocluster with an octahedral Ag <sub>6</sub> <sup>4+</sup> core. Chemical Communications, 2013, 49, 300-302.	2.2	244
59	Surface and interface control of noble metal nanocrystals for catalytic and electrocatalytic applications. Nano Today, 2013, 8, 168-197.	6.2	431
60	Shape transformation from Pt nanocubes to tetrahexahedra with size near 10nm. Electrochemistry Communications, 2012, 22, 61-64.	2.3	44
61	A Multiâ€Yolk–Shell Structured Nanocatalyst Containing Subâ€10 nm Pd Nanoparticles in Porous CeO <sub>2</sub> . ChemCatChem, 2012, 4, 1578-1586.	1.8	75
62	Carbon monoxide-controlled synthesis of surface-clean Pt nanocubes with high electrocatalytic activity. Chemical Communications, 2012, 48, 2758.	2.2	77
63	Selective Hydrogenation of α,βâ€Unsaturated Aldehydes Catalyzed by Amineâ€Capped Platinumâ€Cobalt Nanocrystals. Angewandte Chemie - International Edition, 2012, 51, 3440-3443.	7.2	277
64	Small Adsorbateâ€Assisted Shape Control of Pd and Pt Nanocrystals. Advanced Materials, 2012, 24, 862-879.	11.1	415
65	Carbon monoxide-assisted shape control of Pd and Pt nanocrystals. Scientia Sinica Chimica, 2012, 42, 1525.	0.2	1
66	Small molecules control the formation of Pt nanocrystals: a key role of carbon monoxide in the synthesis of Pt nanocubes. Chemical Communications, 2011, 47, 1039-1041.	2.2	150
67	General and Facile Syntheses of Metal Silicate Porous Hollow Nanostructures. Chemistry - an Asian Journal, 2010, 5, 1439-1444.	1.7	21
68	Interfacial activation of catalytically inert Au (6.7 nm)-Fe3O4 dumbbell nanoparticles for CO oxidation. Nano Research, 2009, 2, 975-983.	5.8	66
69	Nonaqueous Production of Nanostructured Anatase with High-Energy Facets. Journal of the American Chemical Society, 2008, 130, 17563-17567.	6.6	389
70	Electrochemical Reduction of Nitrogen to Ammonia by Pd‣â€Mo Nanosheets on Hydrophobic Hierarchical Graphene Support. ChemElectroChem, 0, , .	1.7	1
71	Low-Temperature Fabrication of Phase-Pure α-FAPbI3 Films by Cation Exchange from Two-Dimensional Perovskites for Solar Cell Applications. Energy & Fuels, 0, , .	2.5	11